Short communication

Carbonaceous anodes for lithium-ion batteries in combination with protic ionic liquids-based electrolytes

Sebastian Menne, Matthias Schroeder, Thomas Vogl, Andrea Balducci*

University of Muenster, MEET Battery Research Centre and Institute of Physical Chemistry, Corrensstr. 28/30, 48149 Münster, Germany

HIGHLIGHTS

- Protic ionic liquids (PILs) are promising electrolyte for lithium-ion batteries.
- Protic ionic liquids display all favorable properties of ionic liquids.
- PILs-based electrolyte can be used in combination with carbonaceous anodes for LIB.

ARTICLE INFO

ABSTRACT

Protic ionic liquids (PILs) have been recently proposed as a new class of electrolytes for lithium-ion batteries (LIBs). So far, PILs-based electrolytes have been used in combination with several battery materials, but never with carbonaceous anodes. Since graphite is the state-of-the-art anode in LIBs, the use of PILs-based electrolyte in combination with this material appears of particular importance. In this work we showed, for the first time, that PILs-based electrolytes can be successfully used also in combination with graphite. Even if the lithium intercalation and deintercalation process of these electrode materials occur outside the ESW of PILs, the addition of film-forming additive makes possible the formation of a stable SEI and, consequently, the use of PILs-based electrolytes. The results of this study indicate that the performance of graphite electrode in PILs-based electrolytes is comparable, and even slightly higher, than that observed in AIL-based electrolytes.

© 2014 Elsevier B.V. All rights reserved.

1. Introduction

Ionic liquids (ILs) display negligible vapor pressure, high chemical and thermal stabilities, high ionic conductivity and large electrochemical stability [1–3]. Thanks to this unique combination of properties ILs are presently regarded as one of the most interesting alternative electrolytes for advanced electrochemical storage devices, including lithium-ion batteries (LIBs). In the last years many types of ILs have been proposed as electrolytes for LIBs and used in combination with several cathodic and anodic materials [4–9]. The results of these studies indicate that the use of ILs might have a positive impact on the safety of LIBs [10]. Nevertheless, they also indicated that further improvements are still necessary for ILs-based LIBs in order to match the performance of the systems containing conventional organic solvents [11,12]. Additionally, also the price of ILs has been indicated as an important obstacle for the introduction of these electrolytes on LIBs.

Graphite is currently the anode of choice in commercial LIBs and its use in combination with electrolytes containing aprotic ionic liquids (AILs) has been widely investigated [13,14]. AILs display rather large cathodic stabilities, which might exceed the lithium plating/stripping potential [14–16]. It has been shown that when these ILs, e.g. N-butyl-N-methylpyrrolidinium bis(trifluoromethane sulfonyl)imide (PYR$_{14}$TFSI), are used in combination with graphite their cation might co-intercalate into the graphite layers, leading to the exfoliation of the graphite itself [17,18]. Therefore, like in conventional electrolytes, the presence of SEI forming components, e.g. VC, EC or the anion of the ILs itself [19–21], appears necessary for a successful use of ILs in combination with graphite electrodes.

Recently, we proposed the use of protic ionic liquids (PILs) as electrolytes for LIBs. We showed that PILs-based electrolytes display good affinity for battery materials and, when dry electrolytes are used, battery materials can be safely used in these protic electrolytes [22,23]. Moreover, we also showed that PILs-based LIBs containing lithium iron phosphate (LFP) as cathode and lithium titanate (LTO) as anode display, at room temperature, promising performance also at high current densities [23]. Taking into account

* Corresponding author.
  E-mail address: andrea.balducci@uni-muenster.de (A. Balducci).

these results, PILs can be therefore regarded as an interesting class of ILs-based electrolytes for LIBs. Additionally, since they are typically cheaper than AILs, their use could be helpful to overcome the cost limitation related to the use of the ILs-based electrolytes. However, in order to be fully competitive with aprotic ILs and conventional electrolytes, the use of PILs should be also extended to systems containing graphite. As a matter of fact, if PILs-based electrolytes could not be used in combination with the state-of-the-art anode, their introduction would be much less appealing.

In this manuscript we report for the first time about the use of PIL-based electrolytes in combination with graphite and soft carbon-based electrodes. The PIL used for this investigation was the *N*-butylpyrrolidinium bis(trifluoromethanesulfonyl)imide (PYR$_{H4}$TFSI). For comparison, also an electrolyte containing the aprotic ionic liquid (AIL) PYR$_{14}$TFSI was considered. For the preparation of both, protic and aprotic electrolytes, LiTFSI (0.5 M) and vinyl ethylene carbonate (VEC) were used as lithium salt and film-forming additive, respectively. Initially, the conductivity, viscosity, electrochemical stability (ESW) and thermal stability of the two electrolytes were considered. Afterward, their use in combination with graphite and soft carbon-based electrodes was investigated using cyclic voltammetry (CVs) and constant current cycling (CC).

2. Experimental

1-Butylpyrrolidine (Aldrich >98%) was distilled directly before use. HCl (37%) and lithium bis(trifluoromethanesulfonyl)imide (LiTFSI), *N*-methylpyrrolidine (>97%) 1-iodobutane (>99%), ethyl acetate (ACS grade, >99.5%), vinyl ethylene carbonate were used as received. *N*-butylpyrrolidinium bis(trifluoromethanesulfonyl) imide (PYR$_{H4}$TFSI) was synthesized following a procedure similar to that described elsewhere [24]. PYR$_{14}$TFSI was synthesized following the procedure described in Ref. [25]. At the end of the synthesis the obtained ILs were dried under vacuum at 60 °C. The water content of the ILs was measured using coulometric Karl−Fisher titration, and was found to be lower than 10 ppm for both ILs. The conductivity and the viscosity of the three investigated electrolytes were evaluated at 20 °C as indicated in Ref. [11].

Electrochemical stability windows of all electrolytes at RT and 60 °C were evaluated in a three-electrode, Swagelok-cell by linear sweep voltammetry (LSV) at 1 mV s^{-1}. The working electrode was a platinum microelectrode (embedded in PEEK; active area = 0.79 mm^2). An activated carbon pellet was used as counter and Ag-wire as reference electrode. The measurements were performed at 20 °C using a Solartron model 1287A potentiostat controlled by Corrware® software. Separate LSV tests were carried out on each sample to determine the cathodic and anodic electrochemical stability limits. The measurements were performed by scanning the cell potential from the open circuit potential (OCP) toward more negative (cathodic limit) or positive (anodic limit) potentials. Clean electrodes and fresh samples were used for each test.

Graphite (SFG6, TIMCAL, Switzerland, specific nitrogen BET surface area: 17 m^2 g^{-1} [26]), soft carbon (Petrol coke, TIMCAL, Switzerland, specific nitrogen BET surface area: 17 m^2 g^{-1} [27]) and carbon-coated LiFePO$_4$ (Südchemie, Germany) as active materials, sodium carboxymethyl cellulose (Walocel CRT 2000, Dow Wolff Cellulosics) and polyvinylidene fluoride (PVdF, Kynar 761) as binders and carbon black (Super C65, TIMCAL) as conductive agent were used as delivered. For preparation of the used anodes, PVdF was dissolved in NMP to obtain a 1.5 wt.% solution and equilibrated for 1 h at room temperature with a magnetic stirrer. The active material (graphite or soft carbon) and conductive agent (Super C65) were added. The anode coating was applied with a doctor blade to a copper foil (dendritic, SCHLENK, Germany). The obtained

electrodes were dried at 100 °C under vacuum. The mass loading of the electrodes was 2 mg. The area was 1.13 cm^2.

All the electrochemical tests were carried out in three-electrode Swagelok® cells. The cells were assembled in a dry box (MBraun) with oxygen and water contents lower than 1 ppm. As separator, a stack of three non-woven fleeces (FS2226, Freudenberg, Germany) drenched with 80 mm^3 of electrolyte was used. As counter electrode an oversized LFP electrodes (ca. 11 mg cm^{-2}) were used.

The electrochemical measurements were carried out using a MACCOR Series 4000 battery tester. Constant current cycling (CC) was carried out at 30 °C using different current densities. Current density corresponding to 1C, was used for the CC investigations. The C-rate was calculated on the base of the theoretical capacity of graphite (372 mA g^{-1}).

3. Results and discussion

Fig. 1 shows the thermal stability of the two investigated (neat) ILs as obtained by thermogravimetric analysis. As shown, PYR$_{14}$TFSI is thermally stable up to almost 400 °C, while the PYR$_{H4}$TFSI up to 300 °C. Most likely, the thermal stability of PYR$_{H4}$TFSI is lower than that of PYR$_{14}$TFSI because of the more reactive protic character of the PILs. Nevertheless, these results clearly indicated that the thermal stability of PILs, as for AILs, is significantly higher than that of conventional organic electrolytes [10–12].

Table 1 compares the conductivity and the viscosity of the PIL-based electrolyte 0.5 M LiTFSI in PYR$_{H4}$TFSI with those of the AIL-based electrolyte 0.5 M LiTFSI in PYR$_{14}$TFSI. As shown, the conductivities of both electrolytes are almost identical (ca. 2 mS cm^{-1}). On the other hand, the viscosities of the two electrolytes are rather different, and the AIL-based electrolyte is more viscous than the PIL-based electrolyte (ca. 30%). This difference might be originated by the lower sterical hindrance cation PYR$_{H4}^+$ compared to that of PYR$_{14}^+$ [28].

Fig. 2 compares the overall ESW of the two electrolytes. As shown, both of them display nearly the same anodic stability, which is above 5.5 V *vs.* Li/Li$^+$. These values are comparable with those reported in literature for other TFSI-based electrolytes [29]. On the other hand, the cathodic stability of the two electrolytes is significantly different. Whilst the stability of 0.5 M LiTFSI in PYR$_{14}$TFSI is exceeding the lithium plating/stripping potential (0 V *vs.* Li/Li$^+$), 0.5 M LiTFSI in PYR$_{H4}$TFSI is electrochemically stable only
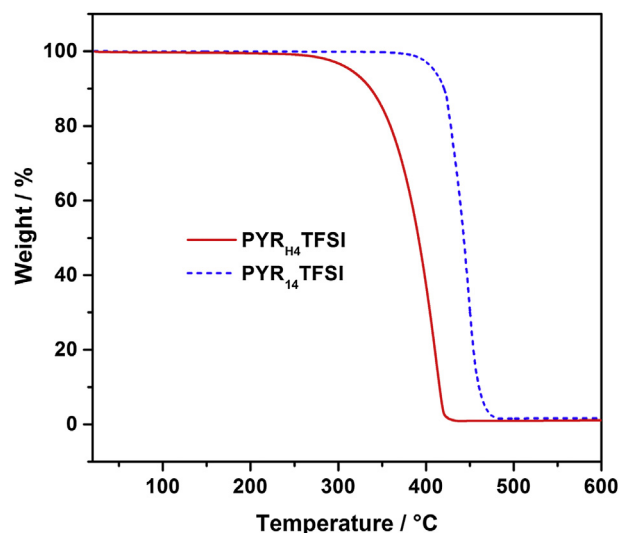

Fig. 1. Thermogravimetric analysis of PYR$_{H4}$TFSI and PYR$_{14}$TFSI in the temperature range from RT to 600 °C.

Electrolyte	Conductivity/mS cm^{-1}	Viscosity/mPa s
0.5 M LiTFSI in PYR$_{H4}$TFSI	2.0	99.7
0.5 M LiTFSI in PYR$_{14}$TFSI	1.9	136.7

till 2.0 V *vs.* Li/Li$^+$. This difference is obviously ascribed to the presence of the proton on the cation PYR$_{H4}^+$, which is reduced below 2 V *vs.* Li/Li$^+$ [24].

Considering the results reported above, it appears evident that the electrolytes 0.5 M LiTFSI in PYR$_{H4}$TFSI and 0.5 M LiTFSI in PYR$_{14}$TFSI display comparable chemical–physical properties, but the ESW of the PILs-based electrolyte results much smaller than that of the AILs-based one. As mentioned in Section 1, when PYR$_{14}$TFSI is used in combination with graphite electrodes, the use of a film-forming agent is needed in order to avoid exfoliation of the graphite electrode, which is caused by the electrochemical stability of the PYR$_{14}$$^+$ cation. In the case of the PYR$_{H4}$TFSI the presence of a film-forming additive seems also to be necessary. In this case, however, such need is originated by the limited cathodic stability of the PYR$_{H4}$$^+$ cation. Considering these points, and with the aim to test both electrolytes in combination with graphite and soft carbon-based electrodes, VEC (2 wt.%) has been added to both electrolytes. As reported in literature, VEC decomposes at a potential around 1.9 V *vs.* Li/Li$^+$. Therefore, the VEC decomposition process is expected to occur inside the ESW of 0.5 M LiTFSI in PYR$_{H4}$TFSI.

Fig. 3 shows a comparison of the cyclic voltammetry of a graphite electrode in 0.5 M LiTFSI in PYR$_{H4}$TFSI + VEC and 0.5 M LiTFSI in PYR$_{14}$TFSI + VEC, as obtained during test carried out using a scan rate of 0.05 mV s^{-1} at room temperature (RT). As shown in the figure, the peaks relative to the insertion of lithium into graphite are visible in both electrolytes, indicating that they can be used in combination with this anodic material. In the inset of Fig. 3 it is visible the peak associated to the VEC decomposition, which
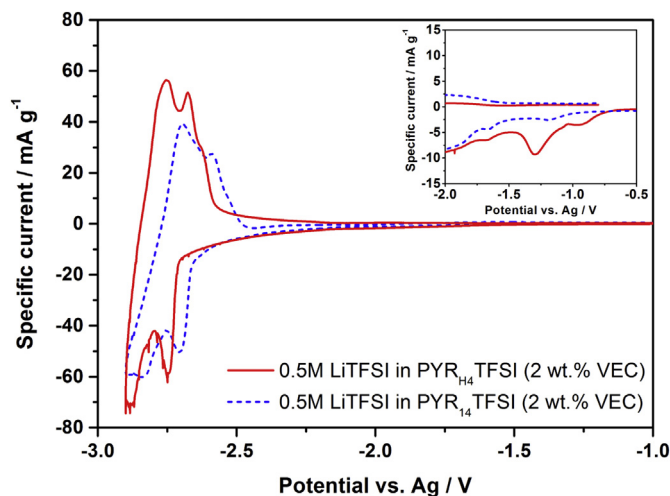

Fig. 3. Cyclic voltammograms of graphite (SFG6) in 0.5 M LiTFSI in PYR$_{H4}$TFSI with 2 wt.% VEC and in 0.5 M LiTFSI in PYR$_{14}$TFSI with 2 wt.% VEC. The insets show the VEC decomposition region during the first cycle.

start around 1 V vs. Ag-wire in both electrolytes. As expected, the VEC decomposition takes place inside the ESW of the PILs-based electrolyte. It is interesting to notice that the peak associated to the decomposition of VEC appears less pronounced in PYR$_{14}$TFSI than in PYR$_{H4}$TFSI, indicating that a different interaction between VEC and the two ILs might be present. Due to the relatively high viscosity and limited conductivity of both electrolytes at RT, the CVs appear less ideal compared to that observed for the same material in conventional electrolyte [30]. This difference has been already reported for many IL-based electrolytes and it is therefore not unexpected [29,31]. Nevertheless, it is interesting to note that in the PIL-based electrolyte the peaks associated to the lithium interaction and deintercalation process result sharper and the current associated with these process is higher compared to that of the AIL-based one. This difference could be associated to the different viscosities of the two electrolytes. Taking into account these results, it appears that when a film-forming agent is added, also PILs-based electrolytes can be used in combination with graphite-based electrode. Additionally, they also indicate that the performance obtained in these electrolytes is similar to that of "traditional" AILs.
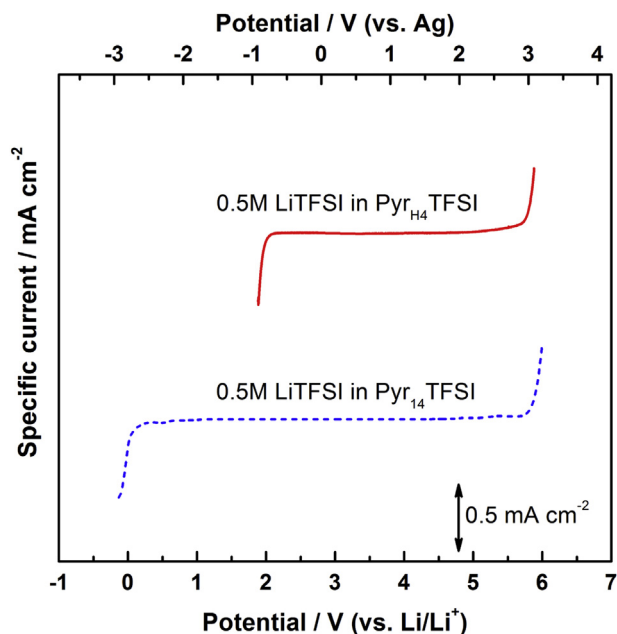

Fig. 2. Electrochemical stability windows (ESW) of the electrolytes 0.5 M LiTFSI in PYR$_{H4}$TFSI and 0.5 M LiTFSI in PYR$_{14}$TFSI. The measurements were done using a silver pseudo-reference. The scale referring to lithium is added for better comparison.
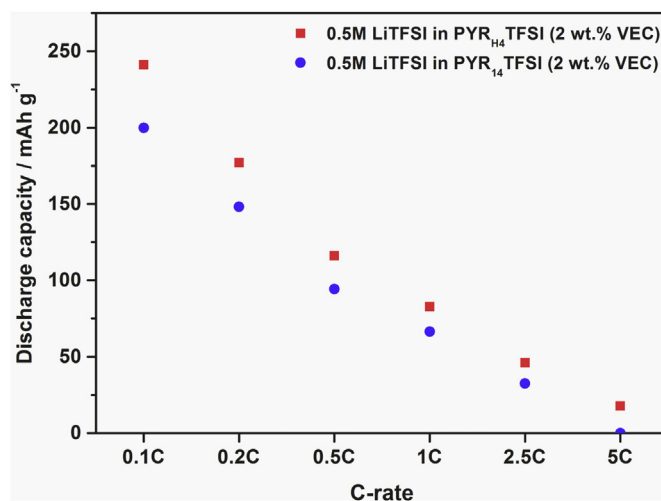

Fig. 4. C-rate test, carried out at RT, of SFG6 graphite electrodes in 0.5 M LiTFSI in PYR$_{H4}$TFSI with 2 wt.% VEC and in 0.5 M LiTFSI in PYR$_{14}$TFSI with 2 wt.% VEC.

Fig. 4 compared the specific discharge capacity of graphite electrodes on the two investigated electrolytes at different C-rates. As shown, when a current density corresponding to 0.1C is applied, the graphite electrode cycled in PIL-based electrolyte display a discharge capacity of about 240 mAh g^{-1}. In the case of the AIL-based electrolyte, the same electrode displays a discharge capacity of about 200 mAh g^{-1}. This difference appears in line with the results observed during the CVs. Recently, we showed that PIL-based electrolytes display higher lithium mobility compared to AIL-based electrolytes [32]. This different lithium mobilities are most likely the origin of the higher initial capacity observed for the graphite electrodes cycled in PIL-based electrolyte [32]. When the C-rate is increased the electrode capacity decreases significantly in both electrodes. Such decrease has been already reported in literature and it is therefore not unexpected. The decrease of capacity is comparable in both electrolytes and, due to its initial higher capacity, the electrode cycled in the PIL-based display at all applied C-rate higher capacity compared to the one tested in the AILs-based electrolyte.

Since the cycling stability is an essential requirement for battery material, also the behavior of the electrodes during prolonged cycles has been investigated. Fig. 5a shows a comparison of variation of the discharge capacity of the investigated electrodes over 20 cycles carried out at 1C. In Fig. 5b the voltage profiles of the two electrodes are reported. As shown, both electrolytes assure a good cycling stability, and the capacity delivered by the graphite
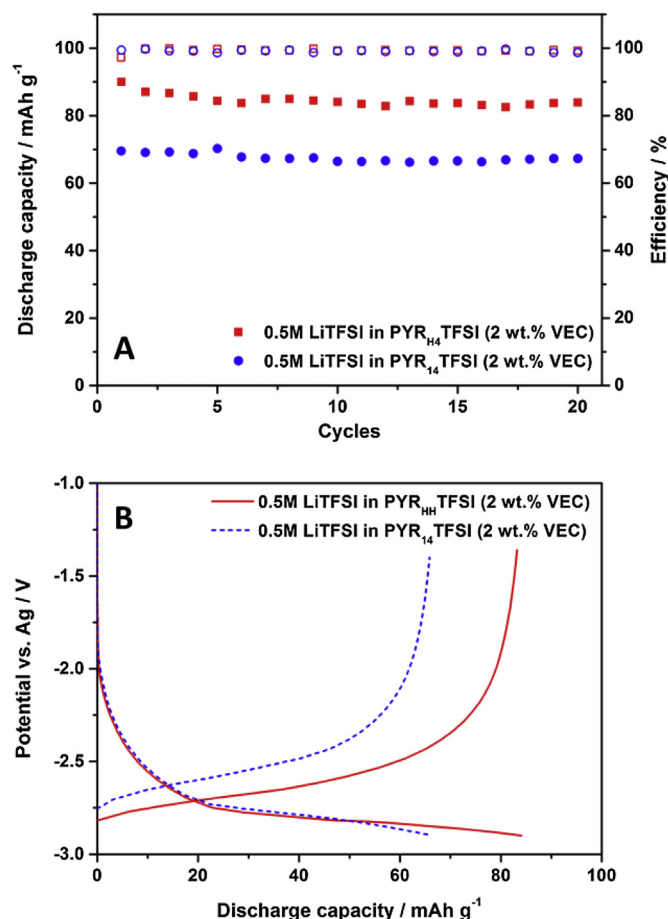

Fig. 6. Cyclic voltammograms of soft carbon (PeC) in 0.5 M LiTFSI in PYR$_{H4}$TFSI with 2 wt.% VEC. The insets show the VEC decomposition region during the first cycle.

electrodes is constant over 20 cycles. Interestingly, at this relative C-rate the capacity delivered by the electrode cycled in 0.5 M LiTFSI in PYR$_{H4}$TFSI (90 mAh g^{-1}) is about 20% higher than that of the electrode cycled in 0.5 M LiTFSI in PYR$_{14}$TFSI (70 mAh g^{-1}). As shown in Fig. 5b, in both electrodes the typical plateau of intercalation and deintercalation of graphite is not well visible. As already mentioned for the CV experiments, this behavior is rather common in IL-based electrolytes and is due to the higher viscosity of these electrolytes compared to that of conventional organic solvents.

Soft carbons have been investigated since many years as anodic materials for LIBs and recently they have been also indicated as promising anodic materials for lithium-ion capacitors [30]. As soft carbons display a more disordered structure and contain more defect than graphite, the irreversible capacity during the first cycles of these materials is typically higher than that of graphite electrodes [27]. Therefore, the formation of a stable SEI appears particularly important for the utilization of this material. It is interesting to note that that in the electrolytes 0.5 M LiTFSI in PYR$_{14}$TFSI it was not possible to cycle soft carbon electrodes (results not shown). To the contrary, it was possible to use soft carbon electrodes in combination with 0.5 M LiTFSI in PYR$_{H4}$TFSI. As shown

Fig. 5. Discharge capacity of SFG6 graphite electrodes in 0.5 M LiTFSI in PYR$_{H4}$TFSI with 2 wt.% VEC and in 0.5 M LiTFSI in PYR$_{14}$TFSI with 2 wt.% VEC. The test was carried at RT using a current density corresponding to 1C (A). Comparison of the voltage profiles (2nd cycle) (B).
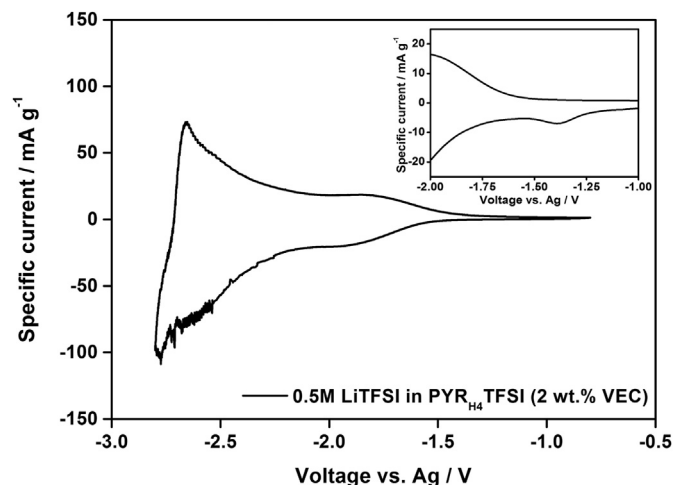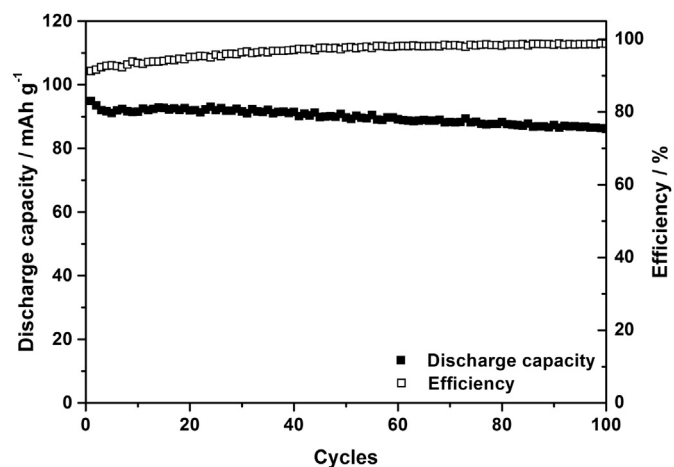

Fig. 7. Discharge capacity of soft carbon (PeC) electrodes in 0.5 M LiTFSI in PYR$_{H4}$TFSI with 2 wt.% VEC. The test was carried out at RT using a current density corresponding to 1C.

in Fig. 6a, the electrode displays the typical voltammetric curves (also in this case the decomposition of VEC was visible but, surprisingly, at −1.4 V *vs.* Ag-wire) as well as the typical voltage profile (Fig. 6b) of soft carbon. Fig. 7 shows prolonged cycling of such a soft carbon electrode at 1C. As shown, the electrode displayed a relative stable capacity (of ca. 90 mAh g^{-1}) for 100 cycles at this current density. Considering these results, PILs-based electrolytes appear to be suitable also with soft carbons.

4. Conclusions

In this work we showed, for the first time, that PILs-based electrolytes can be successfully used also in combination with graphite and soft carbon electrodes. Even if the lithium intercalation and deintercalation process of these electrode materials occurs outside the ESW of PILs, the addition of film-forming additive, e.g. VEC, make possible the formation of a stable SEI and, consequently, the use of PILs-based electrolytes. Moreover, the results of this study indicate that the performance of graphite electrode in PILs-based electrolytes is comparable, and even slightly higher, than that observed in AIL-based electrolytes. Additionally, they also showed that PILs-based electrolytes can be successfully used also in combination with soft carbon, while the use of AILs seems to be, with these materials, more problematic.

In our opinion this investigation can be seen as a proof of concept about the use of PILs-based electrolytes in combination with carbonaceous anodes for LIBs, Certainly, the performance of PIL-based electrolytes in combination with these materials need to be further improved and several aspects related to the use of these innovative electrolytes should be further considered. Among them two appears of particular interest. The first is the investigation of the SEI composition, in order to verify if the proton present of the PIL cation might influence the formation as well as the chemistry of the SEI. The second, is the investigation of ILs containing different cation, e.g. imidazolium-based, or anion, e.g. FSI^{-}, which as it has been shown for AIL-based electrolytes, might have a strong influence on the SEI formation and on the electrode performance.

Acknowledgments

References

[1] M. Armand, F. Endres, D.R. MacFarlane, H. Ohno, B. Scrosati, Nat. Mater. 8 (2009) 621—629.
[2] J.F. Wishart, Energy Environ. Sci. 2 (2009) 956—961.
[3] A. Lewandowski, A. Swiderska-Mocek, J. Power Sources 194 (2009) 601—609.
[4] J. Caja, Kem. Ind. 54 (2005) 205.
[5] B. Garcia, S. Lavallée, G. Perron, C. Michot, M. Armand, Electrochim. Acta 49 (2004) 4583—4588.
[6] M. Holzapfel, C. Jost, A. Prodi-Schwab, F. Krumeich, A. Würsig, H. Buqa, P. Novák, Carbon 43 (2005) 1488—1498.
[7] L. Larush, V. Borgel, E. Markevich, O. Haik, E. Zinigrad, D. Aurbach, G. Semrau, M. Schmidt, J. Power Sources 189 (2009) 217—223.
[8] J. Li, S. Jeong, R. Kloepsch, M. Winter, S. Passerini, J. Power Sources 239 (2013) 490—495.
[9] S. Seki, Y. Kobayashi, H. Miyashiro, Y. Ohno, A. Usami, Y. Mita, N. Kihira, M. Watanabe, N. Terada, J. Phys. Chem. B 110 (2006) 10228—10230.
[10] A. Balducci, S.S. Jeong, G.T. Kim, S. Passerini, M. Winter, M. Schmuck, G.B. Appetecchi, R. Marcilla, D. Mecerreyes, V. Barsukov, V. Khomenko, I. Cantero, I. De Meatza, M. Holzapfel, N. Tran, J. Power Sources 196 (2011) 9719—9730.
[11] R.S. Kühnel, N. Böckenfeld, S. Passerini, M. Winter, A. Balducci, Electrochim. Acta 56 (2011) 4092—4099.
[12] S. Menne, R.S. Kühnel, A. Balducci, Electrochim. Acta 90 (2013) 641—648.
[13] K. Gao, X.-H. Song, Y. Shi, S.-D. Li, Electrochim. Acta 114 (2013) 736—744.
[14] H. Srour, C. Rouault, H. Santini, J. Electrochem. Soc. 160 (2012) A66—A69.
[15] A. Lewandowski, A. Swiderska Mocek, J. Appl. Electrochem 40 (2010) 515—524.
[16] H. Yoon, P.C. Howlett, A.S. Best, M. Forsyth, D.R. MacFarlane, J. Electrochem. Soc. 160 (2013) A1629—A1637.
[17] Y. Katayama, M. Yukumoto, T. Miura, Electrochem. Solid-state Lett. 6 (2003) A96—A97.
[18] Y. Yang, F. Lu, Z. Zhou, W. Song, Q. Chen, X. Ji, Electrochim. Acta 113 (2013) 9—16.
[19] J.P. Boeuve, B. Simon, in, Google Patents, 1997.
[20] H. Ota, Y. Sakata, A. Inoue, S. Yamaguchi, J. Electrochem. Soc. 151 (2004) A1659—A1669.
[21] B.V. Ratnakumar, M.C. Smart, S. Surampudi, J. Power Sources 97—98 (2001) 137—139.
[22] N. Böckenfeld, M. Willeke, J. Pires, M. Anouti, A. Balducci, J. Electrochem. Soc. 160 (2013) A559—A563.
[23] S. Menne, J. Pires, M. Anouti, A. Balducci, Electrochem. Commun. 31 (2013) 39—41.
[24] L. Timperman, P. Skowron, A. Boisset, H. Galiano, D. Lemordant, E. Frackowiak, F. Beguin, M. Anouti, Phys. Chem. Chem. Phys. 14 (2012) 8199—8207.
[25] G.B. Appetecchi, S. Scaccia, C. Tizzani, F. Alessandrini, S. Passerini, J. Electrochem. Soc. 153 (2006) A1685—A1691.
[26] S.R. Sivakkumar, J.Y. Nerkar, A.G. Pandolfo, Electrochim. Acta 55 (2010) 3330—3335.
[27] M. Schroeder, M. Winter, S. Passerini, A. Balducci, J. Electrochem. Soc. 159 (2012) A1240—A1245.
[28] S. Menne, T. Vogl, A. Balducci, Phys. Chem. Chem. Phys. 16 (2014) 5485—5489.
[29] G.B. Appetecchi, M. Montanino, A. Balducci, S.F. Lux, M. Winterb, S. Passerini, J. Power Sources 192 (2009) 599—605.
[30] S.-I. Lee, Y.-S. Kim, H.-S. Chun, Electrochim. Acta 47 (2002) 1055—1067.
[31] S.F. Lux, M. Schmuck, G.B. Appetecchi, S. Passerini, M. Winter, A. Balducci, J. Power Sources 192 (2009) 606—611.
[32] T. Vogl, S. Menne, R.-S. Kühnel, A. Balducci, J. Mater. Chem. A 2 (22) (2014) 8258—8265, http://dx.doi.org/10.1039/C3TA15224C.